DOI: 10.48011/asba.v2i1.1727

Using Differential Evolution Techniques for Management of a Hybrid-Electric Propulsion System ⋆

Manuel A. Rendón * **Carlos D. Sanchez R.** ** **Josselyn Gallo M.** ** **José F. Garcia S.** ** **Ning Xiong** *** **Patricia Habib Hallak** * **Nícolas Lima Oliveira** * **Yipsy Roque Benito** * **Janderson Mazzine Afonso** *

* *Grupo de Conversão Eletromecânica de Energia - GCEME, Federal University of Juiz de Fora - UFJF, Brazil (e-mail: manuel.rendon@ufjf.edu.br, patricia.hallak@ufjf.edu.br, nicolas_limaoliveira@yahoo.com.br, yipsy.benito@engenharia.ufjf.br, janderson.mazzine2015@engenharia.ufjf.br)*
** *Escuela Superior Politécnica del Litoral - ESPOL, Ecuador (e-mail: josesgal@espol.edu.ec, cardasan@espol.edu.ec, jofrgarc@espol.edu.ec)*
*** *Mälardalen University - MDH, Västerås, Sweden (e-mail: ning.xiong@mdh.se)*

Abstract: The air transportation industry contributes with 2% of the total greenhouse gas emissions, and there is a demand from global aviation regulators for reducing this percentage. Hybrid-electric propulsion systems (HEPS) for aircraft is an area of increasing interest for achieving these goals. It is a multidisciplinary research that involves internal combustion engines (ICE), electric motors (EM), power electronic converters, energy storage devices, propeller design, monitoring and control systems, management, etc. The Electromechanical Energy Conversion Group (GCEME) in Brazil developed a complete HEPS test bench and Laboratory. The facility will be able to test three different topologies: Series, full-electric and turbo-electric. The present work employs a detailed model for the test bench, and given a mission profile and the energy consumption as optimization function, it applies Differential Evolution (DE) techniques in the energy management code. The results highlight the nonlinear nature of the HEPS model, and the worth of this methodology in looking for an optimal solution to reduce the computing processing time.

Keywords: Evolutionary algorithms for optimal control, Optimal control of hybrid systems, Real time optimization and control.

1. INTRODUCTION

The term hybrid-electric on aircraft propulsion defines a technology where more than one type of energy source is employed, traditionally fuel/chemical and battery/electrochemical (Sahoo et al., 2020; Assanis et al., 1999). Most HEPS employ internal combustion engines (ICE), which are usually over-sized to meet requirements in certain stages of the flight, which renders high fuel consumption in the whole mission (Assanis et al., 1999). Some studies work on developing management strategies that consider among others to map the advantages of combining HEPS energy sources, to study the overall performance, aiming on saving fuel, reducing emissions and mechanical noise.

Energy management strategies (EMS) can be classified in optimization and rule-based (Zhang et al., 2018). Optimization-based strategies include dynamic programming (DP) (Leite and Voskuijl, 2020), model predictive control (MPC) (Doff-Sotta et al., 2020), and genetic algorithms (GA) (Xie et al., 2020). These strategies succeeded in optimizing fuel consumption, but fail for online management due to the high computational cost. Most of the online strategies published for UAVs are rule-based strategies, mainly fuzzy logic control (FCL) (Dawei et al., 2017), and state machine (SM) (Yang et al., 2018). The results of the aforementioned studies show that it is possible to obtain great improvements in the optimization of the powertrain design, the structure of the aircraft, parameters of the trajectory, etc.

In order to study this technology it is being mounted in Brazil a HEPS test bench made up of several subsystems: gas turbine turbo-generator (GT), EMs, power electronic converters, a battery bank, a propeller, and control and management systems (subsystems will be detailed bellow).

⋆ ESPOL, FAPEMIG and EMBRAER financed the present work.

2. FACILITY DESCRIPTION

The bench is composed by a 32 kW GT, a set of three power electronic converters, a 30 kW battery bank, a 42 kW EM, and a 1.4 m diameter wooden propeller. An electric generator and a resistive load will replace the mechanical load in some tests for safety reasons. The control architecture is observed in Fig. 1.

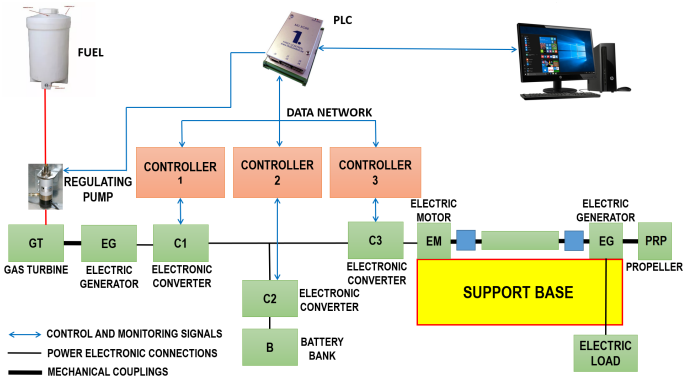

Figure 1. Facility architecture (Rendon et al., 2020).

The fuel employed for the present work was aviation kerosene QAV-1 (PETROBRAS, 2014). Every subsystem was modeled from their physical principles equations, to be later employed by the management code.

3. MODELING DESCRIPTION

Some considerations were adopted in order to simplify the analysis of the concentrated parameter model: (i) no energy dissipation occurs in the fuel tank and batteries; (ii) batteries have constant specific energy; (iii) steady state is considered for every subsystem; (iv) gravity does not change with increasing altitude; and (v) the aircraft lift-to-drag ratio is considered constant. SI units were employed in the model equations.

3.1 Turbo-Generator

The GT dynamic model is based on the balance equations of specific enthalpy and entropy. Ideal gas modelling was employed for obtaining the properties of air and combustion gases for temperatures from 200 K to 3300 K (Bücker et al., 2003). No dissociation effects were considered. Pressures and temperatures in the gas path were calculated from enthalpy and entropy relations (Kyprianidis et al., 2012). Three fluids were considered, the initial dry air, the fuel and the combustion gas. The fuel for this analysis was aviation kerosene, and the chemical composition of these three fluids were the same.

Compressor and turbine maps were obtained from (Gimelli and Sannino, 2017). Sampled data was employed to validate the model (Rendón, 2010).

A feedback control loop regulates the power generated by the GT through a Proportional-Integral (PI) control law with variable reference shaft speed.

3.2 Power Electronic Converters

The electronic converters were modelled from physical principles (Nascimento et al., 2019; Torres et al., 2019).

Rectifier

The implemented rectifier receives the power from the high frequency permanent magnet synchronous generator (PMSG) of the GT. Using p-q transformation to control the active and reactive power, maintains a DC reference voltage of 670 V_{DC} at the rectifier output. It employs a PI control law in the external loop, and a proportional compensator plus resonant for the internal current control loop, in order to make a real resonant control, eliminate the infinite gain margin and avoid stability problems.

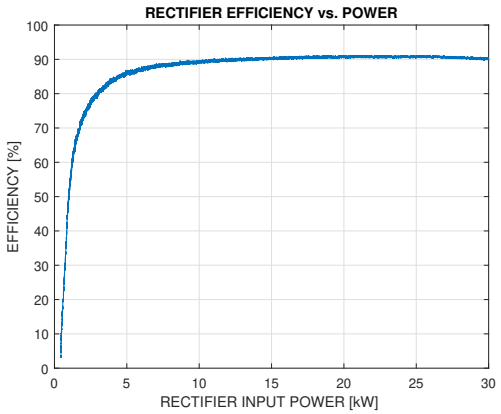

Figure 2. Rectifier efficiency vs. input power

Active power losses influence the global management, the variation of efficiency with operation condition is presented in Figure 2. Losses in the IGBTs switching due to the internal resistance affect the performance and efficiency of the rectifier, that will vary with the power that it is supplying.

As observed in Figure 2, it is now worth to work in power under 2500 W. It just starts to have acceptable value around 80%, and from 6000 W it reaches above 90%. From this value onwards the efficiency begins to increase a little, with a maximum around 91.5%. This variable efficiency characterizes a non-linear system. Figure 3 presents the rectifier circuit in Matlab.

Interleaved Bidirectional DC-DC Converter

For commanding the battery supplying power, an interleaved DC-DC converter was used (Figure 6). It was designed to work in buck (charge) or boost (discharge) modes. Three branches were employed to divide the current, and the analysis was done for a single branch.

The converter operates in three different conditions. In the first one, a control loop adjusts the battery discharge current, supplying energy to the DC bar. In the second, the same control loop adjusts the battery charge current, obtaining the energy from the DC bar. In these two conditions a PI control law was employed. The reference current was calculated by the management system, with signal for charging the opposite than for discharging. In the third condition the DC voltage is adjusted in 670 V_{DC} through a control loop using a PI control law. In

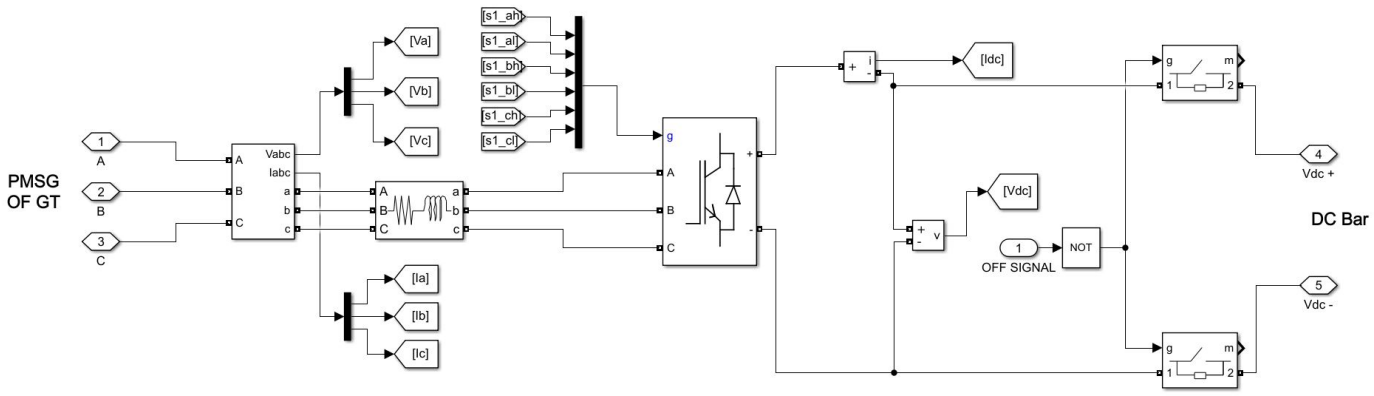

Figure 3. Three-phase rectifier diagram.

this situation the controller calculates the reference current necessary to keep the required voltage.

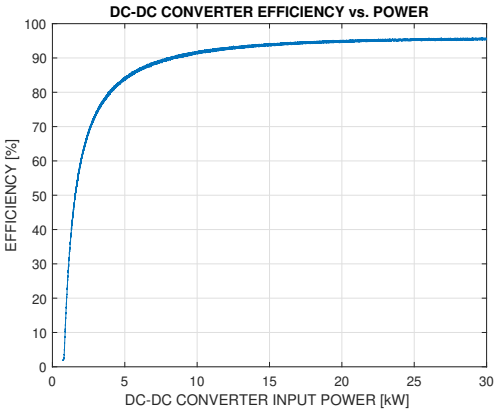

Figure 4. DC-DC Converter efficiency vs. input power

The DC-DC converter also have losses with similar behavior to the rectifier. Figure 4 shows that from 7500 W the efficiency will have a high value and from this power onwards, it will gradually increase until reaching an efficiency limit of approximately 96%. That is, the efficiency for low power is even less than the rectifier, but at high power the efficiency is greater.

Inverter and Electrical Motor

The power electronics inverter uses an (integral-proportional) IP control law to adjust the EM shaft speed, using the output electrical frequency as the manipulated variable. The EM is a 42 kW, 380 V, three-phase permanent magnet synchronous motor (PMSM), which drives the propeller. The characteristics of the motor are detailed in the Table 1. i_d and i_q axes currents, and they are monitored with an IP approach, that unlike traditional PI controllers, does not add a pole in zero in the closed-loop transfer function, and therefore there will be no oscillations in steady state. The inverter is the most efficient of the three converters, as seen in Figure 5. From 2000 W the efficiency is higher than 90% and thereafter it keeps increasing for higher powers, reaching a maximum of 97%.

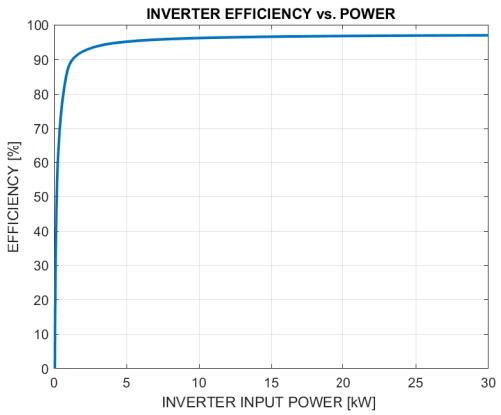

Figure 5. Inverter efficiency vs. input power

Table 1. Parameters of Electrical Motor

Symbol	Name	Value
R_s	Phase resistance	18 $m\Omega$
L_d	Direct axis inductance	175 μH
L_q	Quadrature axis inductance	180 μH
Z_p	Number of pairs of poles	10
J_m	EM inertia	0.0421 Kg.m^2
B_v	Viscous damping	0.005 N.m.s
ϕ_{pm}	Axial magnetic flux	0.0542 V.s

3.3 Battery Bank

The batteries used are lithium polymer with a nominal capacity of 40 A-h, an operating voltage between 2.8 V and 4.0 V, and a weight of 1.6 kg each. For modeling in the Matlab-Simulink application it was used the "Battery" block, and the parameters were adjusted to obtain the voltage vs. discharge capacity curve near the one supplied by the manufacturer. 78 of these batteries are connected in series, and a curve was calculated to represent these parameters in the model (Figure 7). The battery bank owns a nominal voltage of 250 V_{DC}, and a power of 30 kW.

3.4 Propeller

Propeller efficiency and thrust equations are borrowed from previous analysis that employed blade element momentum theory and computational fluid dynamics (Rocha,

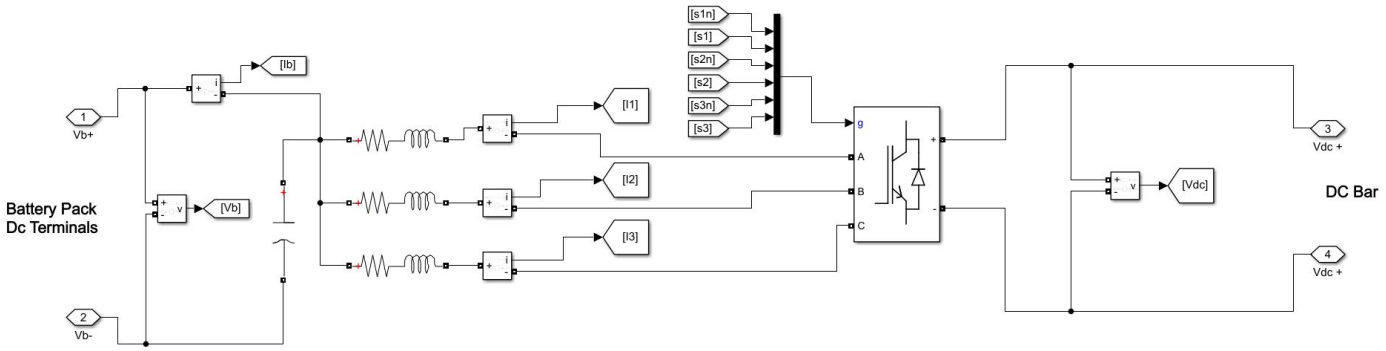

Figure 6. Interleaved Bidirectional DC-DC Converter diagram.

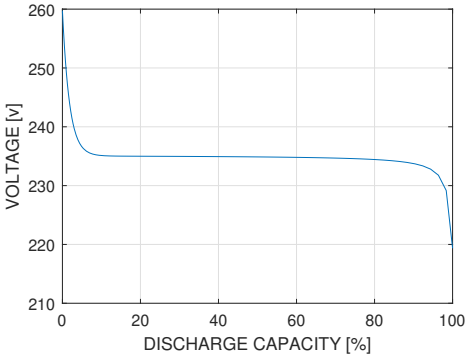

Figure 7. Battery bank Voltage vs. Discharge capacity

2019; Oliveira et al., 2019). The propeller is modelled by equations (1)–(4).

$$\eta_{PRP} = -4.48 \cdot 10^{-10} \cdot \dot{W}_{PRP}^2 + 3.03 \cdot 10^{-5} \cdot \dot{W}_{PRP} + 0.2688 \quad (1)$$

$$\dot{W}_{PRP_{out}} = \eta_{PRP} \cdot \dot{W}_{PRP} \quad (2)$$

$$\tau_{PRP} = \frac{\dot{W}_{PRP}}{n_{PRP}} \quad (3)$$

$$T = 2.84 \cdot 10^{-6} \cdot \dot{W}_{PRP_{out}}^2 - 0.091 \cdot \dot{W}_{PRP_{out}} + 1124 \quad (4)$$

The equations (1)–(4) were fitted through results obtained from an application developed in ANSYS CFX software. The propeller dimensions were obtained to construct the application, meshes around $500k$ elements and faces that are inferior than $512k$ were considered. Simulations from 200 to 3000 *rpm* were performed, with a step of 400 *rpm*. The results are plotted on Figure 8. The velocity streamline is displayed on Figure 9.

- Open conditions with zero gauge pressure were used on the front, back and side faces;
- No slip wall conditions were used on the floor face nor on any of the faces that form the structural base. No slip wall conditions were used on propeller and axis faces;
- Frozen rotor domains were used to generate the rotation of axis and propeller;
- k-ω SST turbulence model and air proprieties at 25 ^{o}C were used.

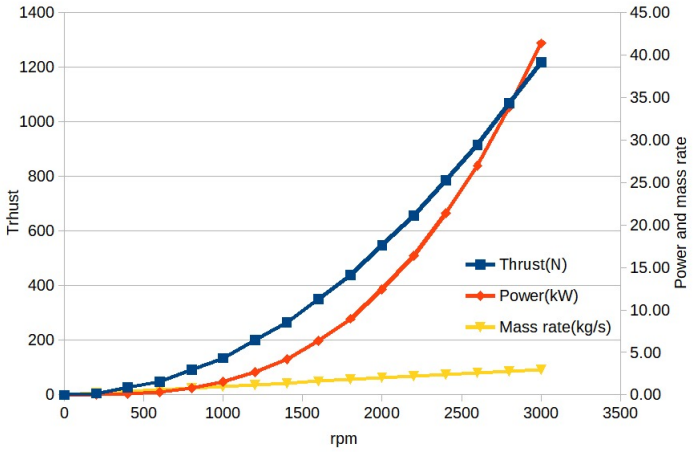

Figure 8. Thrust, Power and Mass Rate vs. Shaft Speed in *rpm*

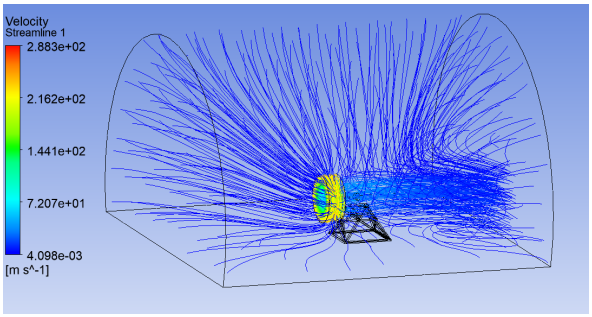

Figure 9. Velocities streamline from ANSYS application

3.5 Aircraft

Some aircraft characteristics were tested in the simulation and are related in Table 2.

Some key values are computed in equations (5)–(9). ESAR relates the distance traveled by the aircraft with the total power employed (Friedrich and Robertson, 2015). The hybridization ratio Γ (Buecherl et al., 2009) shows the relationship between the amount of electric power used, compared with the total power. The energy use ratio β (Schmitz and Hornung, 2013) is used to measure the ratio of the electrical energy supplied by the battery to the total energy of the system. In this work the power sources where fuel and batteries.

Table 2. Aircraft Parameters

Description	Symbol	Value	Units
Fuel heating value	FHV	42.8	$\frac{MJ}{kg}$
Lift-to-drag ratio	L_D	12	–
Aircraft mass	m_{ACF}	240	kg
Battery bank mass	m_{BAT}	125	kg
Electric motor mass	m_{EM}	12.3	kg
Fuel mass in the reservoir	m_{FUE}	40	kg
Propeller mass	m_{PRP}	3	kg
GT mass	m_{ICE}	40	kg
Aircraft velocity in climb stage	V	28	$\frac{m}{s}$
Aircraft velocity in cruise and descent	V	35.44	$\frac{m}{s}$

$$\eta_{ACF} = \frac{\dot{W}_{PRP_{out}}}{\dot{W}_{FUE} + \dot{W}_{BAT}} \tag{5}$$

$$P_p = \frac{\dot{W}_{FUE} + \dot{W}_{BAT}}{T} \tag{6}$$

$$ESAR = \frac{V \cdot L_D}{P_p \cdot m_{ACF}} \tag{7}$$

$$\beta = \frac{E_{BAT}}{E_{FUE} + E_{BAT}} \tag{8}$$

$$\Gamma = \frac{\dot{W}_{BAT}}{\dot{W}_{FUE} + \dot{W}_{BAT}} \tag{9}$$

4. MANAGEMENT OF THE HEPS

The management system aims to optimize the HEPS energy consumption. Energy flows from the fuel and batteries, through the GT and power electronics, to the EM and propeller. The management determines which is the optimal hybridization strategy. Variables such as climb angle, descent angle, and a factor of recharge of the batteries are analyzed. References control values for control loops in GT power/speed, and electronic converters are defined from the management code.

The management code uses equations with variable efficiencies for each subsystem. In order to reduce the computational time, detailed models described before are substituted by polynomial equations in steady state conditions.

Differential Evolution (DE) is a population-based technique from the Evolutionary Algorithm family. It has become popular due to its strength and easiness in solving optimization problems (Leon, 2019). Given the characteristics of the problem addressed in this study this technique was chosen because it promises to render the global optimum results in the shorter computing time, and also due to its simplicity. Several mutation strategies on DE were tested, and the results are presented in the end.

4.1 Differential Evolution

DE was proposed in 1995 to be used for optimization problems (Storn et al., 1995). It was developed to improve an algorithm based on Goldberg Genetic Algorithms and Simulated Annealing, aiming to achieve greater speed, robustness and simple structure (Echevarría et al., 2014).

When seeking to optimize non-linear or non-differentiable problems direct search methods are preferred, because they are based on variations of the initial vectors. Once this variation is made, they go through a selection stage to accept or not to accept these variations, since they may or may not improve the objective function. This decision process usually converges fairly quickly, but there is a risk of converging to local optimal points (Storn et al., 1995). The method employed allows obtaining a rapid convergence in an effective global minimum, with few parameters to control.

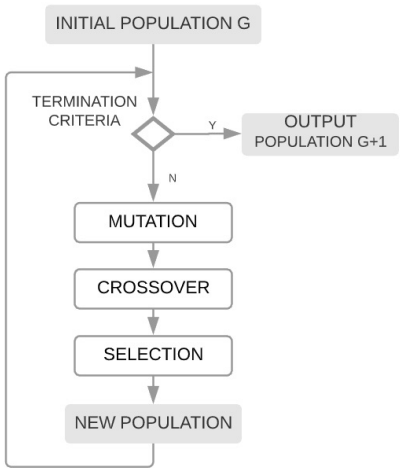

Figure 10. Differential Evolution Algorithm

DE consists of an initial population with m individuals, in which each individual in that population contains a number n of variables, which represent the inputs of the system to optimize (angle of rise, angle of descent and recharge factor of the batteries). Each individual will go through three stages called: mutation, crossing and selection (Figure 10). The equations can be found in (Leon, 2019). This three-step cycle is carried out until the algorithm's completion criterion is met: (i) it reaches a maximum number of iterations and (ii) until there are no significant improvements in the function to be optimized or a minimum is reached expected.

Mutation: At this stage, after creating the initial population randomly, each individual goes through any of the 6 mutation forms (Leon, 2019). Where F represents the mutation factor, a value between 0 and 2 and V corresponds to the new (mutated) vector.

Crossover: In this stage, three variables are used: (i) The crossover rate RC, which refers to how permissive the change of the initial individuals is. (ii) A random number $R1$ between 0 and 1. (iii) A random integer number $randIndex$, between 1 and n and allows the vector resulting from the crossing (U) since the change of at least one position of the initial vector X.

Selection: In this stage, a comparison is made between the evaluation in the objective function of the initial randomly generated vector and the vector resulting from the crossing; the individual with the lowest evaluation is selected.

5. RESULTS

A profile mission was simulated to test the DE code with energy consumption as the function cost. A fixed-wing Unmanned Aerial Vehicle (UAV) is commanded to travel along a trajectory, where the initial and final destinations are 600 km apart from each other. Figure 11 depicts the flight profile. It encompasses the three stages of the mission: Climb, Cruise, and Descent. Climb and descend angles vary from $\theta = 15°$ to $\theta = 45°$. The velocities in Fig. 11 are kept constant in each phase independent of the angles.

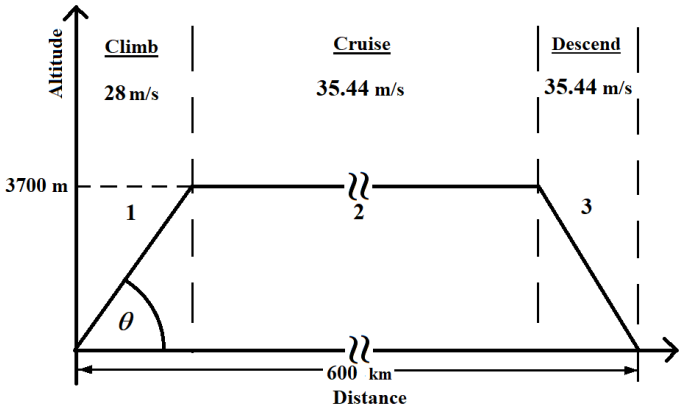

Figure 11. Mission Profile

Five simulations were performed to analyze the contribution of variables such as the climb/descent angle, and the fraction of battery recharge p. Due to the low energy density of batteries related with fuel, in cruise stage the batteries must be charged/discharged several times along the stage. The last variable is a number between 0 and 1 that represents the fraction of battery energy that is allowed to discharge until the correspondent recharging. In the last simulation it was observed the benefit of using DE in terms of computing time.

The first one simulates an aircraft with only the GT to power the propulsion. The angles of climb and descent were varied to find the optimal condition that minimizes the energy consumption. Electronic converters and battery pack were not considered, as well as their related weights and power losses. Additional weight was considered due to the mechanical speed reducer, and the additional fuel needed to complete the mission. The results are shown in the Table 3.

Table 3. Optimal condition for an aircraft powered with GT

Simulation Time	N/A
Climb angle	15°
Descent angle	45°
p	N/A
f(X)	2.0614 x 10^9 (J)

The following three simulations are linear search approaches.

The second simulation (Figure 12.) consists of a linear search for the best fraction of battery recharge and the best climb/descent angle (equal climb and descent angles were considered). The results are observed in Figure 12. The optimal condition is shown in Table 4 as well as the energy consumption and computing time. The energy consumption is clearly lower than using only the GT for propulsion.

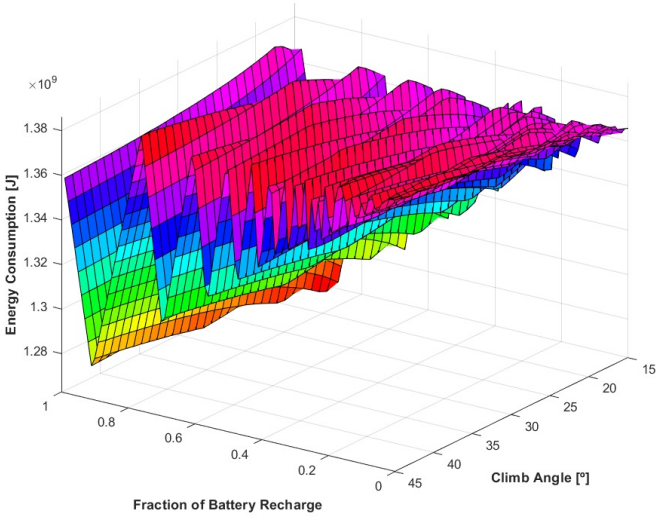

Figure 12. Second Simulation - Surface of Energy Consumption

Table 4. Second Simulation - Optimal condition

Simulation Time	460.5 (s)
Climb angle	16°
Descent angle	16°
p	0.11
f(X)	1.2628 x 10^9 (J)

The third simulation fixes the optimal fraction of battery recharge p calculated in the previous tests, and a linear search evaluates all the possible climb and descent angles combinations. Results are observed in Figure 13. The optimal condition is shown in Table 5. The code converged to a condition with the lower climb angle and the higher descent angle.

Table 5. Third Simulation - Optimal condition

Simulation Time	401.2 (s)
Climb angle	15°
Descent angle	45°
p	0.11
f(X)	1.2365 x 10^9 (J)

There is a reduction in energy consumption related with previous simulations, but not so relevant as related with the first simulation. If we consider the combined time of second and third simulations, we have a total linear search time of 861.7 s.

The fourth simulation is a linear search that tests all the possible combinations of the three variables: climb and descend angles, and fraction of battery recharge p. The optimal solution is presented in Table 6.

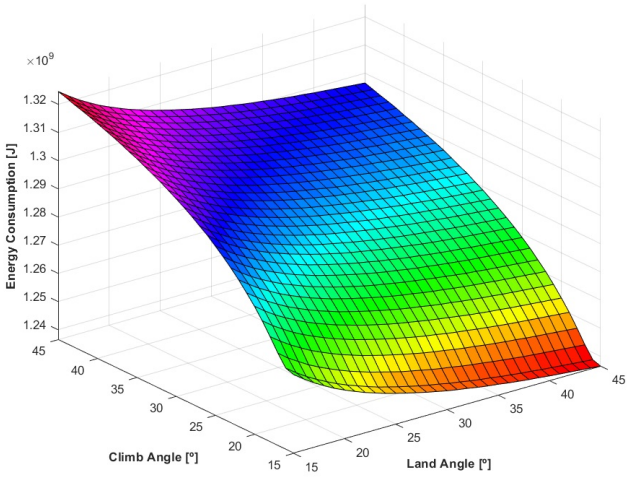

Figure 13. Third Simulation - Surface of Energy Consumption

Table 6. Fourth Simulation - Optimal condition

Simulation Time	3581.7 (s)
Climb angle	15°
Descent angle	45°
p	0.11
f(X)	1.2365×10^9 (J)

The optimal solution found in the fourth simulation is the same as in the third, but the computing time is much bigger as previewed.

The fifth simulation is where the DE code is tested, aiming to perform a faster calculation of the optimal point. The number of variables n is 3 (climb and descent angle, and fraction of battery recharge p), and the population number m is 50. The first population is randomly generated in the range of values (angles from 15° to 45° with variations of 1°, and p from 0 to 0.99 with variations of 0.01). After evaluated the cost function of all the elements of the first population, it is mutated and sent to the selection stage, where the individuals with the best characteristics become part of the next population. This iterative process is carried out until attained the completion criteria: A maximum number of iterations have been met, or the cost function improvement of the optimal individual is under a predefined value.

For the implementation of DE, six mutation methods were used (Leon, 2019), and a comparison was made between 8 strategies as possible ways of varying the mutation-crossing-selection process. This simulation was carried out 10 times and the best individual of each strategy was selected and shown in Table 7. In the first strategy it was used the first mutation method, in the second one the second mutation method and so on, until the sixth strategy. The seventh strategy varies the mutation method sequentially in each iteration (from the first to the sixth), for each individual analyzed. The eighth strategy varies the mutation method randomly for each individual. This process was carried out in order to find the strategy that employs the lower computing time.

Table 7 shows the results of applying this technique. Most of the DE strategies present a computing time around the half of the employed in the linear search (second and third simulations). The best strategy attains a computing time four times lower than the linear search method, with the same optimal solution.

6. CONCLUSIONS

Savings in energy consumption using a HEP system in aircraft propulsion are relevant compared with traditional GT powered systems. The use of well developed management and optimization algorithms even increases its natural advantages.

HEPS is a complex system composed by several subsystems, each one of them with non-linear relations between their energy variables. Management of this system is a task that demands a detailed and accurate modeling of each subsystem. Steady-state relations of the input and output energy variables were used to replace the complex models, initially by interpolations and later by polynomial equations. Results showed that this approach reduced the computing times.

Even with this the processing time still high as shown, and evolutionary techniques were tested to improve this parameter. Six mutation methods in eight DE strategies were tested. The results showed that strategy number three gave better results, with rapid convergence to the optimal solution. The fourth strategy presented a similar behavior. Strategies three and four use the "best individual", that is the one who has the lowest evaluation in the objective function of each population This characteristic seems to shorten the search space in this particular application.

Future studies will consider more input variables, including hybridization ratio and aircraft velocity, and other techniques will be tested. When the HEP test bench is mounted and operating, real data will be used to adjust sub-system models, and the best management techniques will be tested and validated.

ACKNOWLEDGMENT

The authors would like to thank the Institutions ESPOL, UFJF, and FAPEMIG, for supporting actual research. Also, to the EMBRAER Technical Development Board, for the partnership that enabled the advancement in the exploration of technical/scientific knowledge.

REFERENCES

Assanis, D., Delagrammatikas, G., Fellini, R., Filipi, Z., Liedtke, J., Michelena, N., Papalambros, P., Reyes, D., Rosenbaum, D., Sales, A., et al. (1999). Optimization approach to hybrid electric propulsion system design. *Journal of Structural Mechanics*, 27(4), 393–421.

Bücker, D., Span, R., and Wagner, W. (2003). Thermodynamic property models for moist air and combustion gases. *J. Eng. Gas Turbines Power*, 125(1), 374–384.

Buecherl, D., Bolvashenkov, I., and Herzog, H. (2009). Verification of the optimum hybridization factor as design parameter of hybrid electric vehicles. In *2009 IEEE Vehicle Power and Propulsion Conference*, 847–851. doi:10.1109/VPPC.2009.5289758.

Table 7. Evaluation of the Differential Evolution Strategies

DE strategies	Iteration	Simulation Time (s)	Climb Angle (°)	Descent Angle (°)	p	f(X) (J)
Strategy 1	11	470.359	15	42	0.11	1.2350×10^9
Strategy 2	9	242.836	15	45	0.11	1.2354×10^9
Strategy 3	4	197.399	15	45	0.11	1.2300×10^9
Strategy 4	5	223.205	15	45	0.11	1.2333×10^9
Strategy 5	22	934.689	15	38	0.11	1.2354×10^9
Strategy 6	7	530.240	15	42	0.11	1.2349×10^9
Strategy 7	14	283.141	15	38	0.11	1.2364×10^9
Strategy 8	10	324.399	15	45	0.11	1.2339×10^9

Dawei, M., Yu, Z., Meilan, Z., and Risha, N. (2017). Intelligent fuzzy energy management research for a uniaxial parallel hybrid electric vehicle. *Computers & Electrical Engineering*, 58, 447–464.

Doff-Sotta, M., Cannon, M., and Bacic, M. (2020). Optimal energy management for hybrid electric aircraft. *arXiv preprint arXiv:2004.02582*.

Echevarría, L.C., Santiago, O.L., and da Silva Neto, A.J. (2014). Aplicación de los algoritmos evolución diferencial y colisión de partículas al diagnóstico de fallos en sistemas industriales. *Investigación Operacional*, 33(2), 160–172.

Friedrich, C. and Robertson, P. (2015). Hybrid-electric propulsion for automotive and aviation applications. *CEAS Aeronaut J*, 1(6), 279–290. doi: 10.1115/1.4025066. URL `https://doi.org/10.1007/s13272-014-0144-x`.

Gimelli, A. and Sannino, R. (2017). Thermodynamic model validation of capstone c30 micro gas turbine. In *Proceedings of the 72^{nd} Conference of the Italian Thermal Machines Engineering Association (ATI2017) — Italia*, volume 126, 955–962.

Kyprianidis, K.G., Sethi, V., Ogaji, S., Pilidis, P., Singh, R., and Kalfas, A. (2012). Uncertainty in gas turbine thermo-fluid modelling and its impact on performance calculations and emissions predictions at aircraft system level. *Proceedings of the Institution of Mechanical Engineers, Part G: Journal of Aerospace Engineering*, 226(2), 163–181.

Leite, J.P.S.P. and Voskuijl, M. (2020). Optimal energy management for hybrid-electric aircraft. *Aircraft Engineering and Aerospace Technology*.

Leon, M. (2019). Improving differential evolution with adaptive and local search methods. Mälardalen University Doctoral Dissertation.

Nascimento, S.O., Vinicius, M., Fernandes, M.d.C., Rendón, M.A., Oliveira, J.G., and Almeida, P.S. (2019). Modeling and control of a back-to-back system for turboelectric propulsion. In *2019 IEEE 15th Brazilian Power Electronics Conference and 5th IEEE Southern Power Electronics Conference (COBEP/SPEC)*, 1–6. IEEE.

Oliveira, N.L., Rocha, L.M., Hallak, P.H., and Rendón, M.A. (2019). Influence of crosswinds on propellers performance. In *25^a ABCEM International Congress of Mechanical Engineering (COBEM)*. ABCM.

PETROBRAS (2014). *Querosene de Aviação, Informações Técnicas p.4*. Petróleo Brasileiro S. A., 1.3 edition. `http://sites.petrobras.com.br/minisite/assistenciatecnica/public/downloads/QAV-Informações-Técnicas-v.1.3-29.pdf`.

Rendón, M.A. (2010). *Desenvolvimento de Modelos Matemáticos Representativos do Comportamento Dinâmico de Micro-Turbinas para a Conexão na Rede Elétrica*. Ph.D. thesis, Federal University of Itajubá - UNIFEI, Av. BPS 1303, Itajubá, MG, Brazil.

Rendon, M.A., Kyprianidis, K., Roque B., Y., Fernandes, D.d.A., Ferraz, A.T., and Vieira, L.R.C. (2020). Energy management of a hybrid-electric aeronautical propulsion system to be used in a stationanry test bench. In *Proceedings of the ASME TURBO EXPO 2020*.

Rocha, L.M. (2019). *Estudo e Dimensionamento de Hélices para Propulsão Aeronáutica (in Portuguese)*. Master's thesis, Federal University of Juiz de Fora, Juiz de Fora, Brazil.

Sahoo, S., Zhao, X., and Kyprianidis, K. (2020). A review of concepts, benefits, and challenges for future electrical propulsion-based aircraft. *Aerospace*, 7(4), 44.

Schmitz, O. and Hornung, M. (2013). Unified Applicable Propulsion System Performance Metrics. *Journal of Engineering for Gas Turbines and Power*, 135(11). doi: 10.1115/1.4025066. URL `https://doi.org/10.1115/1.4025066`. 111201.

Storn, R., Price, K., et al. (1995). Differential evolution–a simple and efficient adaptive scheme for global optimization over continuous spaces: technical report tr-95-012. *International Computer Science, Berkeley, California*.

Torres, V.C., Vinicius, M., Rendón, M.A., Almeida, P.S., Oliveira, J.G., and Rodrigues, M.C. (2019). Interleaved bidirectional dc-dc converter for application in hybrid propulsion system: Modeling and control. In *2019 IEEE 15th Brazilian Power Electronics Conference and 5th IEEE Southern Power Electronics Conference (COBEP/SPEC)*, 1–6. IEEE.

Xie, Y., Antonios, T., Dan, Z., Jason, G., et al. (2020). Review of hybrid electric powered aircraft, its conceptual design and energy management methodologies. *Chinese Journal of Aeronautics*.

Yang, Z., Lei, T., Lin, Z., Fu, H., and Zhang, X. (2018). The testing platform of hybrid electric power system for a fuel cell unmanned aerial vehicle. In *2018 IEEE International Conference on Electrical Systems for Aircraft, Railway, Ship Propulsion and Road Vehicles & International Transportation Electrification Conference (ESARS-ITEC)*, 1–8. IEEE.

Zhang, X., Liu, L., and Dai, Y. (2018). Fuzzy state machine energy management strategy for hybrid electric uavs with pv/fuel cell/battery power system. *International Journal of Aerospace Engineering*, 2018.